sciendo

Slovak Journal of Civil Engineering

Vol. 31, 2023, No. 4, 9 – 15
DOI: 10.2478/sjce-2023-0022

BEHAVIOR OF AN EMBANKMENT ON STONE COLUMN-REINFORCED SOFT SOIL

Tadesse Abebe, WASSIE[1*] , Gökhan, DEMIR[1]

Abstract

Reinforcing soft soils with good drainage and load-bearing material is a common practice in the construction of embankments. Stone columns are among the granular materials that accelerate consolidation settlements due to their high drainage capacities. This study aims to investigate the behavior of an embankment on stone column-reinforced soft soil. The embankment was analyzed using the Plaxis 2D Finite Element Method. The columns were converted into equivalent walls using the plane strain conversion method. This method was validated with field measurement results from previous studies and showed good agreement. According to the research findings, stone columns significantly reduced deformations and improved consolidation. For instance, the ultimate settlement was decreased from 54.3 mm to 33.1 mm for 10% and 20% area replacement ratios, respectively. As the safety analysis verified, basal geosynthetics contributed substantially to the embankment's stability. Furthermore, the safety factor values increased for all stages of the construction, and the global safety factor increased at the end of the construction. Stone columns and basal geogrid-reinforced soft soil can reduce settlement and increase the stability of an embankment.

Address

[1] Dept. of Civil Engineering, Ondokuz Mayis University, Samsun, Türkiye

* ***Corresponding author:*** tadegeo68@yahoo.com

Key words

- Embankment,
- Plaxis 2D Finite Element Method,
- Safety Factor,
- Soft Soil,
- Stone Columns.

1 INTRODUCTION

Geotechnical structures founded on soft soil require significant attention due to their high water content, low shear strength, low permeability, and unique structural features. Excessive compressibility is a characteristic of soils with undrained shear strength below 15 kN/m^2. Moreover, applying too much structural weight to weak ground can generate excess pore pressure and lead to significant deformations. Buildings constructed on soft soils are prone to excessive deformation and slope failure, particularly deep-seated failure (Deshpande et al., 2021). As land values continue to rise and suitable sites for construction become scarce, engineers look in situ improvement of weak soil deposits.Various ground improvement techniques have been employed to use marginal areas to construct buildings and other infrastructure. Among these techniques, stone columns have proven to be effective and reliable (Dheerendra et al., 2013).

Stone columns are commonly employed to enhance the load-bearing capacity of weak soil and minimize the subsidence of buildings constructed on them. Their analysis and design are typically based on simplified empirical rules, which consider the results of model experiments, on-site tests performed on individual stone columns, and previous experience (Lee and Pande, 1998). Stone columns are extensively used to improve soft clay deposits by increasing bearing capacity,

© 2023 The Author(s). This is an open access article licensed under the Creative Commons Attribution 4 .0 License (https://creativecommons.org/licenses/by/4.0/)

accelerating consolidation, and controlling settlements (Gu et al., 2022; Zheng et al., 2020). They are also frequently used as a partial replacement for rapid embankment construction on a soft soil layer. This is because stone columns have a high degree of permeability and stiffness values, which allow for faster dissipation of excess pore pressure and help accelerate consolidation in the soft soil layer (Tan et al., 2008).

The stone column technique has gained significant attention as a ground improvement method for rapidly constructing embankments on soft soil (Yoo, 2010). Stone columns are an effective method to enhance soft soils due to two crucial factors. Firstly, they involve using a stiffer column material, such as crushed stones or gravel placed within the soft soil. Secondly, when a stone column is installed, it densifies the surrounding soft soil, followed by consolidation (Guetif et al., 2007).

Many scholars have proposed using stone columns to increase soil stability and reduce settlements in soft soils (Alkhorshid et al., 2021; Deb et al., 2011; Bailappanavar et al., 2021; Choobbasti et al., 2011; Belayneh, 2020; Etezad et al., 2015; Almeida et al., 2018; Muzammil et al., 2018). Using stone columns and basal geogrids can reduce subsoil deformations and improve the stability of embankments (Ghorbani et al., 2021).

This study examines the behavior of an embankment constructed on soft soil reinforced with multiple columns. The analytic method allows us to estimate settlement and stress distributions at any location beneath the embankment. The aproach was the axisymmetric-to-plain strain conversion method proposed by (Ng and Tan, 2015). A road embankment supported by several stone columns was analyzed using the 2D finite element method. The axisymmetric column diameter was considered as the plane-strain column width and kept the center-to-center distance of the columns constant. Additionally, the equivalent plane-strain permeability was calculated based on correlation equations.

2 PLAIN STRAIN CONVERSION

(Ng and Tan, 2015) proposed two strategies for transforming the equivalent plane-strain model from the axisymmetric unit-cell model. Both approaches retain the distance between stone columns, while introducing an expanded shear wall for each stone column. In the first approach, the soil permeability varies according to the correlation equations, and the wall's width is the same as the stone column's diameter. Nevertheless, for the second approach, the wall's width is minimized, while the permeability of the soil materials remains unchanged. For modeling linear-elastic material, both techniques yield reasonably realistic long-term consolidation settlements. In this study, the first method proposed by (Ng and Tan, 2015) is applied to analyze an embankment on stone column-reinforced soft soil.

It is feasible to consider the diameter of the axisymmetric column (r_c) to be equal to the plane-strain column's width (b_c) as shown in Fig. 1 (a and b), i.e.:

$$b_c = r_c \tag{1}$$

As a result,the equivalent plane-strain width (B) could be the same as the radius of the drainage zone (R), i.e. :

$$R = B \tag{2}$$

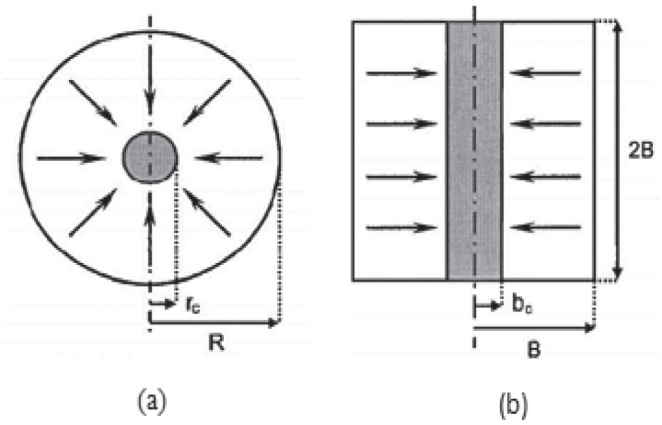


Fig. 1 *Axisymmetric to plain strain conversion (Tan et al., 2008) ; (a) axisymmetric (b) Plain strain*

This method enables a smooth transition from an axisymmetric to a plane-strain conversion. The plane-strain material's properties must be modified to consider the geometric modifications. The following equation, which matches the stiffness of the column-soil composite, provides the plane-strain material's stiffness.

$$E_{c,pl}\, a_{s,pl} E_{s,pl}\left(1 - a_{s,pl}\right) = E_{c,ax} a_{s,ax} + E_{s,ax}\left(1 - a_{s,ax}\right) \tag{3}$$

where, E_s and E_c are elastic moduli of the surrounding soil and the column material, respectively. Additionally, the subscripts *ax* and *pl* denote axisymmetric and plain-strain conditions, respectively.The area replacement ratio is given by $a_s = A_c/(A_c + A_s)$, where A_s and A_c are cross-sectional areas of the surrounding soil and column, respectively.

The following analytical equation is used to match the soil permeability as derived by (Tan et al., 2008):

$$\frac{k_{h,pl}}{k_{h,ax}} = \frac{F(N)_{pl}}{F(N)_{ax}} \left[\frac{m_{vs} m_{vs}(1-a_s)}{m_{vs}(1-a_s)+m_{vs}a_s}\right] pl \left[\frac{m_{vc}(1-a_s)+m_{vs}a_s}{m_{vs}m_{vc}(1-a_s)}\right] ax \frac{B^2}{R^2} \tag{4}$$

where k_h = coefficient of soil permeability in the horizontal direction:

$$F(N) = \left[\frac{N}{N^2-1}\right] \ln(N) - (3N^2 - 1)/(4N^2) \tag{5}$$

Diameter ratio for axisymmetric condition:

$$N = R/r_c \tag{6}$$

Diameter ratio for the plane-strain condition:

$$N = B/b_c \tag{7}$$

$$m_{vs} = (a_{vs})/(1 + e_s) \tag{8}$$

$$m_{vc} = \left(\frac{a_{vc)}}{1+e_c}\right) \tag{9}$$

where a_{vc} and a_{vs} are coefficients of the compressibility of the column and the surrounding soil, respectively, e_c and e_s are the void ratios of the columns and the surrounding soil, respectively. It is anticipated that the plane-strain coefficient of the soil

permeability in the vertical direction, kv, pl, will have little effect on the overall consolidation rate because the movement of water in the soil is mainly radial or horizontal, i.e., $k_{v,pl} = k_{v,ax}$.

3 VALIDATION OF THE MODEL

In this study, the findings of the field measurement results were used to verify the reliability of the 2D finite element model. The settlement of the actual embankment at selected points and the excess pore pressures developed at various spots in the soft soil was measured, as reported by (Tan et al., 2008). As depicted in Fig. 2, the pore pressures were recorded at the *A*, *B*, and *C* locations, and the settlements were measured at the settlement plates 1 and 2. In addition, the embankment had a side slope of 1V-2H, a height of 1.8 m, and a base width of 40 m.The 80 cm diameter stone columns were arranged in a square grid with 2.4 m center-to-center spacing, extending 6 m below the ground's surface. In order to facilitate construction activities on the soft soil and enhance drainage, a layer of dense, granular soil 1 m thick was added on top of the soft clay.

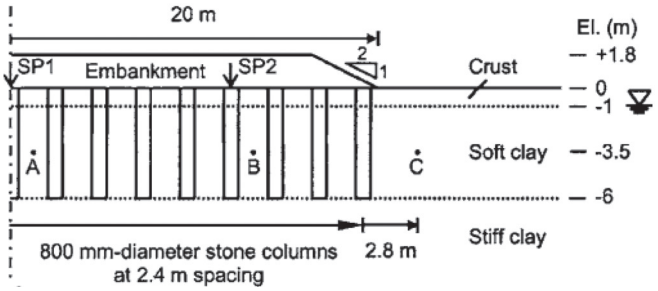


Fig. 2 *An actual embankment in Malaysia, 2003 (Tan et al., 2008)*

The geotechnical engineering program, Finite Element Package (Plaxis 2D V21), was used to analyze the behavior of an embankment on soft soil. Several researchers have extensively used it to analyze various geotechnical problems (Rajesh and Jain, 2015; Lo et al., 2010; Hataf et al., 2020). As stated in Tab. 1, the input parameters for the soil layers, stone columns, and embankment fill were adopted from a previous researcher. The Mohr-Coulomb material model was used for the road embankment, soil layers, and stone columns. The Mohr-Coulomb model is a linear elastic-plastic model that requires five input parameters to describe stress-strain behavior. This model is frequently used because it has a simple formulation and requires less input data from basic tests, making it more applicable than other models. Nevertheless, a linear elastic material property was considered for the basal geosynthetic material.

The model was meshed with a fine-mesh using triangular elements with 15 nodes, as shown in Fig.3, and divided into 619 elements and 5127 nodes. The numerical analysis requires only half of the embankment section to be considered due to the axial symmetry at the center. To verify the model, the embankment's geometry, settlement plate positions, pore pressure locations, clay layer dimensions, and stone column dimensions are identical to those reported by (Tan et al., 2008). The embankment was constructed in three phases, with each step requiring three days to place the 60 cm-thick fill. As a result, the embankment took nine days to finish and reached a height of 1.8 m. After the loading, the embankment was entirely constructed; a consolidation study was performed; and the computations were continued until the excess pore water pressure had completely dissipated. The flow boundary condition was open at the right boundary and at the top of the crust layer and closed at the left boundary and the bottom of the stiff clay layer. The drainage along the left boundary was closed because half of the construction was simulated.

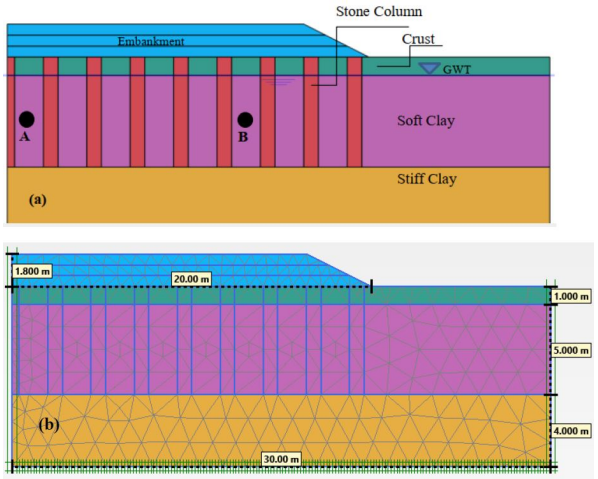
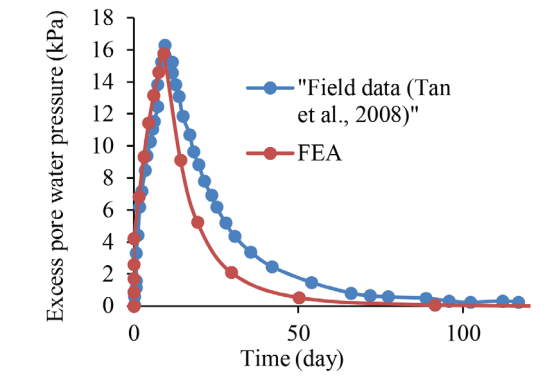


Fig. 3 *Validation of the model; (a) Numerical model used for the analysis (b) Generation of the mesh*

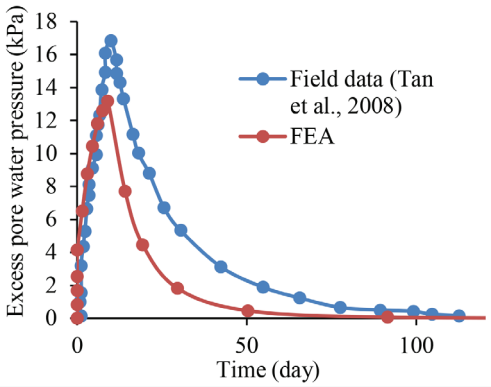
The excess pore water pressure values from the field measurements at sites A and B, see Fig. 3, were compared against the numerical analysis to demonstrate the model's viability. As demonstrated in Fig. 4, the outcomes of the numerical results showed good agreement with the field measurement results. Therefore, the computed numerical model is valid for a further analysis of the different parameters. Fig. 5 depicts the variations of the simulated and measured settlements over time for a position beneath the centerline of the embankment at (0, 0). It is evident that the numerical analysis follows the trend of the results measured and makes relatively accurate predictions.

Tab. 1 *Input parameters for the numerical analysis (After [(Ng and Tan, 2015)]*

Material	γ_{unsat} (kN/m^3)	γ_{sat} (kN/m^3)	ν'	E (kPa)	k_h (m/s)	k_v (m/s)	*c* (kPa)	ϕ (°)
Stone column	19	20	0.3	8,670	$1.16*10^{-4}$	$1.16*10^{-4}$	5	40
Stiff clay	18	20	0.3	40,000	$3.47*10^{-9}$	$1.16*10^{-9}$	3	30
Soft clay	15	15	0.3	1,100	$1.68*10^{-9}$	$1.16*10^{-9}$	1	20
Crust	17	18	0.3	15,000	$3.47*10^{-7}$	$1.16*10^{-7}$	3	28
Road Embankment	18	20	0.3	15,000	$1.16*10^{-5}$	$1.16*10^{-5}$	3	33



(a) Measurements at A



(b) Measurements at B

Fig. 4 *Field and FEA of the pore pressures at points A and B*

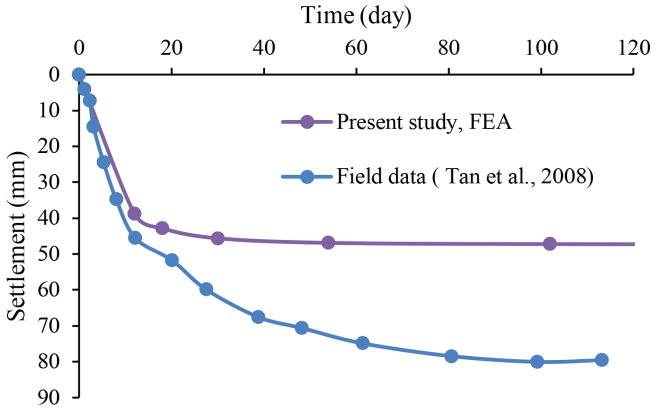


Fig. 5 *Settlement variations at point (0,0) for the numerical analysis and field measurements*

4 PARAMETRIC ANALYSIS

Variables such as the area replacement ratio (a_s), length of the stone columns (L_s), and basal geogrid stiffness (J) were considered when analyzing the road embankment. The values of each parameter are given in Tab. 2.The embankment was built in three stages, each requiring three days to construct the 1.2 m thick fill material. As a result, the embankment took nine days to finish and reached a height of 3.6 m. Following the completion of loading, i.e, the complete construction of the embankment, a consolidation study was carried out, and the calculations were continued until the excess pore water pressure had completely dissipated.

The embankment had a base width of 50 m, a height of 3.6 m, and a side slope of 1V-2H. The actual embankment's stone column diameter, spacing, and slope remained unchanged. The stiff clay was 9 meters deep, as illustrated in Fig. 6, and the total depth of the soil strata in this inquiry was 15 meters. The numerical model shown in Fig. 6 is a new model adopted by altering several geometric dimensions from the initial numerical model used for the validation. The height of the embankment was increased to 3.6 m to improve its performance and clarify the effect of the geogrid on the parametric analysis. Moreover, the mesh's coarseness impacted the pore water pressure and consolidation settlement. Since fine mesh has a higher degree of accuracy (Tan et al., 2008), it was chosen for the numerical analysis of this study.

Tab. 2 *Variables for the parametric analysis*

Variables		Units
Area replacement ratio, a_s(%)	10% (2.3)*, 15% (1.8)*, 20% (1.6)*	m
Length of stone column	0.5 H_s, 0.75 H_s, H_s*	m
Basal geogrid stiffness	3500	kN/m

* Center-to-center column spacing, H_s*Height of soft soil layer

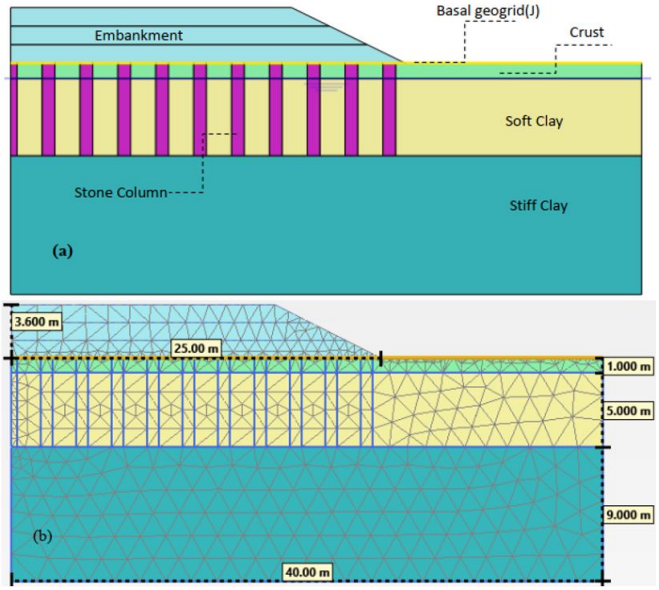


Fig. 6 *The numerical model adopted for the parametric studies and mesh generated*

5 RESULTS AND DISCUSSIONS

5.1 Effect of the area replacement ratio (a_s)

The relationship between the column area (A_c) and its area of influence (A_E) is known as the area replacement ratio ($a_s = A_c/A_E$). Equation (10) is used to compute the area of inf-

luence A_E. The values of the diameter of the area of influence (d_e) are taken as 1.05s (for a triangular mesh), 1.13s (for a square mesh), and 1.29s (for a hexagonal mesh), where "s" is the spacing between the columns (Almeida et al., 2018).

$$A_E = \pi \frac{d_e^2}{4} \tag{10}$$

The stone column spacing (s) of 2.4 m, which is similar to the actual embankment, was used for the finite element analysis on a square mesh. The settlement of the embankment decreases as the area replacement ratio increases, as shown in Fig. 7. After 100 days, the settlement measurements were as follows: 54.28 mm, 36.20 mm, and 33.12 mm for 10%, 15%, and 20% area replacement ratios, respectively. The bearing capacity of a single or group of stone columns increases, and the settlement reduces with increasing the area replacement ratio (Fattah et al., 2017; Nav et al., 2020).

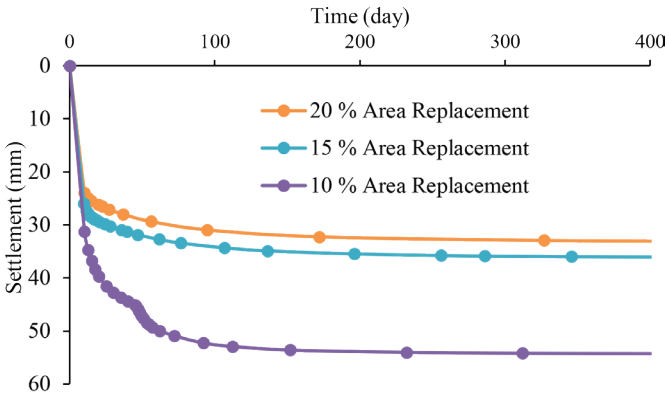


Fig. 7 *Effects of the area replacement ratio on the settlement*

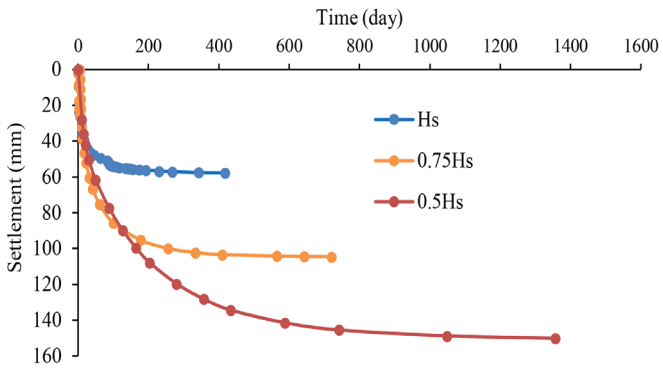


Fig. 8 *Effect of variations of the length of the stone column on settlement*

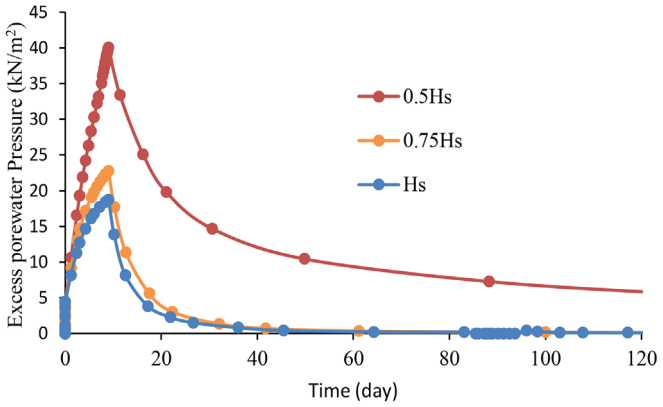


Fig. 9 *Variation of the pore water pressure in the middle of the soft soil layer*

5.2 Effects of the length of the stone columns (L_s)

The length of the stone columns varies, based on the thickness of soft clay (H_s), as indicated in Tab. 2. The diameter and spacing remained constant at 0.8 and 2.4 meters, respectively. A stone-column-reinforced embankment was analyzed to avoid failure. The length of the stone columns affected the settlement of the road embankment, as depicted in Fig. 8. It is evident from the figure that changing the length of the stone columns affected both the heave at the embankment toe and the settlement beneath the embankment. For instance, the maximum settlement would be dropped from 150 mm to 57 mm if the column's length was increased from $0.5H_s$ to H_s. The bearing capacity was improved, and the settlement was reduced when the length of the stone column increased (Ali et al., 2011).

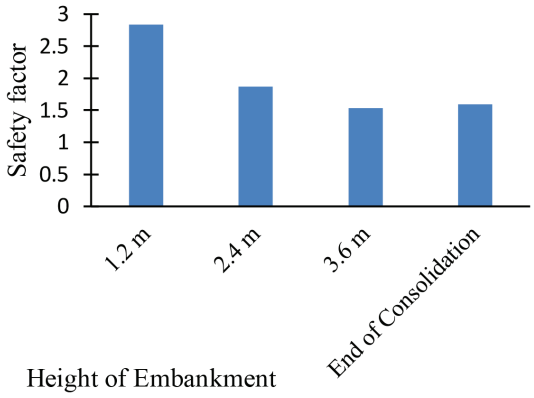
Additionally, Fig. 8 demonstrates how a longer stone column length speeds up the consolidation process and decreases the time needed for the ultimate settlement. The dissipation time, for instance, is decreased from 588 to 45 days by increasing the stone column's length from $0.5H_s$ to H_s. Furthermore, increasing the length of the stone columns from $0.5H_s$ to H_s reduces the maximum pore pressure from 40 to 19 kPa (a 52.5% decrease), as shown in Fig. 9.

5.3 Effects of the stiffness of the basal geogrid (J)

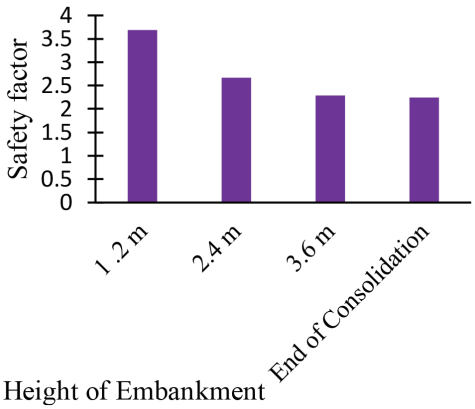
A strength reduction method was carried out for determining the safety factor during the three successive stage constructions. The height of the embankment is 3.6 m, and it is constructed in three consecutive stages. Each stage was allowed to consolidate for three days, and a safety analysis was conducted at the end of each construction stage. As depicted in Fig. 10, the safety factor decreases as the stage construction increases. The safety factor analysis was conducted for an untreated and a basal geosynthetic-treated embankment having a stiffness value (J = 3500 kN/m). Basal geogrid-reinforced embankments have a considerably higher safety factor than unreinforced embankments for each stage of construction and the global safety factor analysis, as demonstrated in Fig. 10. Using a basal geogrid reinforcement in embankments helps to decrease lateral displacements and improves overall stability (Liu etal., 2007).

6 CONCLUSIONS

The behavior of an embankment reinforced with a basal geogrid and supported by stone columns was studied using the plain strain conversion method. Following the model's validation, parametric studies were conducted to determine the effect of the area replacement ratio, stone column length, and basal



(a) Reinforced stone column



(b) Reinforced stone column and basal geogrid

Fig. 10 *Safety factor for stage constructions of the embankment*

geogrid's stiffness on the embankment's behavior. The following conclusions can be drawn from the numerical analysis:

- The settlement reduces when the area replacement ratio increases. For example, the settlement decreases from 54.28 mm to 33.12 mm after 100 days when the area replacement ratio rises from 10% to 20%.
- The increase in the length of the stone column notably reduces settlement and excessive pore water pressure. As the length of the stone column increases from 0.5 times the height of the embankment to the full height of the embankment, there is a decrease in excess pore water pressure from 40 kPa to 19 kPa. It is worth noting that the length of a stone column can affect the settlement beneath the embankment and the heave at the embankment toe. By increasing the column length from $0.5H_s$ to H_s, the maximum settlement of a road embankment built on soft soil was reduced from 150 mm to 57 mm.
- Based on the results of the stability analysis, it was observed that using basal geosynthetics during all the construction phases led to an increase in the embankment's stability. The safety factor at the end of consolidation increased from 1.6 to 2.3 due to reinforcing the road embankment with the basal geogrid.
- In general, the increase in the area replacement ratio, the length of the stone column and the reinforcement of the road embankment at the bottom reduces the settlement and increases the stability of the embankment. This study was conducted for soft soil with a maximum depth of 6 meters. Further studies are recommended for deeper soft soils.

REFERENCES

Ali, K. - Shahu, J. T. - Sharma, K. G. (2011) *An experimental study of stone columns in soft soils.* Proceedings of Indian Geotechnical Conference, 375–378.

Alkhorshid, N. R. - Araujo, G. L. S. - Palmeira, E. M. (2021) *Consolidation of soft clay foundation improved by geosynthetic-reinforced granular columns: Numerical evaluation.* Journal of Rock Mechanics and Geotechnical Engineering, 13(5), 1173–1181. https://doi.org/10.1016/j.jrmge.2021.03.004

Almeida, M. de S. S. de - Filho, M. V. R. - Babaei, I. H. - Alexiew, D. (2018) *Geosynthetic Encased Columns for Soft Soil Improvement. Geosynthetic Encased Columns for Soft Soil Improvement.* CRC Press. https://doi.org/10.1201/9781315177144

Bailappanavar, N. I. - Kumar, M. - Chatterjee, K. (2021). *Effect of Stone Columns on Strength and Consolidation Characteristics of Black Cotton Soil.* KSCE Journal of Civil Engineering, 25(4), 1214–1228. https://doi.org/10.1007/s12205-021-0863-6

Belayneh, H. L. (2020) *The Behavior of Ordinary and Geosynthetic Encased Stone Columns in Collapsible Soil : A Numerical Study,* Global Scientific Journals, 8(12), 978–1004.

Choobbasti, A. J. - Zahmatkesh, A. - Noorzad, R. (2011) *Performance of Stone Columns in Soft Clay: Numerical Evaluation.* Geotechnical and Geological Engineering, 29(5), 675–684. https://doi.org/10.1007/s10706-011-9409-x

Deb, K. - Samadhiya, N. K. - Namdeo, J. B. (2011) *Laboratory model studies on unreinforced and geogrid-reinforced sand bed over stone column-improved soft clay.* Geotextiles and Geomembranes, 29(2), 190–196. https://doi.org/10.1016/j.geotexmem.2010.06.004

Deshpande, T. D. - Kumar, S. - Begum, G. - Basha, S. A. K. - Rao, B. H. (2021) *Analysis of Railway Embankment Supported with Geosynthetic-Encased Stone Columns in Soft Clays: A Case Study.* International Journal of Geosynthetics and Ground Engineering, 7(2). https://doi.org/10.1007/s40891-021-00288-5

Dheerendra Babu, M. R. - Nayak, S. - Shivashankar, R. (2013) *A Critical Review of Construction, Analysis and Behaviour of Stone Columns.* Geotechnical and Geological Engineering, 31(1), 1–22. https://doi.org/10.1007/s10706-012-9555-9

Etezad, M. - Hanna, A. M. - Ayadat, T. (2015) *Bearing Capacity of a Group of Stone Columns in Soft Soil.* International Journal of Geomechanics, 15(2), 04014043. https://doi.org/10.1061/(asce)gm.1943-5622.0000393

Fattah, M. Y. - Al-Neami, M. A. - Shamel Al-Suhaily, A. (2017) *Estimation of bearing capacity of floating group of stone columns.* Engineering Science and Technology, an International Journal, 20(3), 1166–1172. https://doi.org/10.1016/j.jestch.2017.03.005

Ghorbani, A. - Hosseinpour, I. - Shormage, M. (2021) *Deformation and Stability Analysis of Embankment over Stone Column-Strengthened Soft Ground.* KSCE Journal of Civil Engineering, 25(2), 404–416. https://doi.org/10.1007/s12205-020-0349-y

Gu, M. - Mo, H. - Qiu, J. - Yuan, J. - Xia, Q. (2022) *Behavior of floating stone columns reinforced with geogrid encasement in model tests.* Frontiers in Materials, 9 (Aug.), 1–10. https://doi.org/10.3389/fmats.2022.980851

Guetif, Z. - Bouassida, M. - Debats, J. M. (2007) *Improved soft clay characteristics due to stone column installation.* Computers and Geotechnics, 34(2), 104–111. https://doi.org/10.1016/j.compgeo.2006.09.008

Hataf, N. - Nabipour, N. - Sadr, A. (2020) *Experimental and numerical study on the bearing capacity of encased stone columns.* International Journal of Geo-Engineering, 11(1). https://doi.org/10.1186/s40703-020-00111-6

Lee, J. S. - Pande, G. N. (1998) *Analysis of stone-column reinforced foundations.* International Journal for Numerical and Analytical Methods in Geomechanics, 22(12), 1001–1020. https://doi.org/10.1002/(SICI)1096-9853(199812)22:12<1001::AID-NAG955>3.0.CO;2-I

Liu, H. L. - Ng, C. W. W. - Fei, K. (2007) *Performance of a Geogrid-Reinforced and Pile- Supported Highway Embankment over Soft Clay: Case Study.* Journal of Geotechnical and Geoenvironmental Engineering, 133(12), 1483–1493. https://doi.org/10.1061/(asce)1090-0241(2007)133:12(1483)

Lo, S. R. - Zhang, R. - Mak, J. (2010) *Geosynthetic-encased stone columns in soft clay: A numerical study.* Geotextiles and Geomembranes, 28(3), 292–302. https://doi.org/10.1016/j.geotexmem.2009.09.015

Muzammil, S. P. - Varghese, R. M. - Joseph, J. (2018) *Numerical Simulation of the Response of Geosynthetic Encased Stone Columns Under Oil Storage Tank.* International Journal of Geosynthetics and Ground Engineering, 4(1), 1–12.https://doi.org/10.1007/s40891-017-0122-6

Nav, M. A. - Rahnavard, R. - Noorzad, A. - Napolitano, R. (2020) *Numerical evaluation of the behavior of ordinary and reinforced stone columns.* Structures, 25, 481–490. https://doi.org/10.1016/j.istruc.2020.03.021

Ng, K. S. - Tan, S. A. (2015) *Stress Transfer Mechanism in 2D and 3D Unit Cell Models for Stone Column Improved Ground.* International Journal of Geosynthetics and Ground Engineering, 1(1), 1–9. https://doi.org/10.1007/s40891-014-0003-1

Rajesh, S. - Jain, P. (2015) *Influence of permeability of soft clay on the efficiency of stone columns and geosynthetic-encased stone columns - A numerical study.* International Journal of Geotechnical Engineering, 9(5), 483–493. https://doi.org/10.1179/1939787914Y.0000000088

Tan, S. A. - Tjahyono, S. - Oo, K. K. (2008) *Simplified Plane-Strain Modeling of Stone- Column Reinforced Ground.* Journal of Geotechnical and Geoenvironmental Engineering, Vol. 134, 185–194. https://doi.org/10.1061/ASCE1090-02412008134:2185

Yoo, C. (2010) *Performance of Geosynthetic-Encased Stone Columns in Embankment Construction: Numerical Investigation.* Journal of Geotechnical and Geoenvironmental Engineering, 136(8), 1148–1160. https://doi.org/10.1061/(asce)gt.1943-5606.0000316

Zheng, G. - Yu, X. - Zhou, H. - Wang, S. - Zhao, J. - He, X. - Yang, X. (2020) *Stability analysis of stone column-supported and geosynthetic-reinforced embankments on soft ground.* Geotextiles and Geomembranes, 48(3), 349–356. https://doi.org/10.1016/j.geotexmem.2019.12.006